# Calibration of anaerobic digestion BioModel by using multi-objective optimization and full-scale biogas plant data

Tina Kegl
*Faculty of Chemistry and Chemical Engineering*
*University of Maribor*
Maribor, Slovenia
tina.kegl@um.si

***Abstract***

**Waste management and energy crisis are some of the greatest issues that the world is facing today. This problem can be mitigated by anaerobic digestion (AD), where microorganisms in the absence of oxygen produce biogas from organic waste. A useful tool for AD process understanding and optimization is numerical simulation by using mechanistically inspired mathematical models. In this paper attention is focused on modeling of the AD process of a full-scale biogas plant. Special attention is focused on calibration of 178 model parameters belonging to the BioModel, developed in-house; this is done by using an active set optimization procedure. The agreement of the obtained results of numerical simulation in a single CSTR and the measured AD performance over a period of one year, confirms the efficiently of the used BioModel when considering the presence of the Kemira BDP-840 additive to reduce $H_2S$ content of the produced biogas. The obtained results show that the active set optimization procedure, coupled by a gradient based optimizer to calibrate the model parameters, performs very well. The procedure is numerically efficient, especially if the computation of design derivatives is parallelized. The used BioModel can easily be coupled with the procedure of AD performance optimization.**

***Keywords: Model parameters, calibration, additives, gradient-based optimization, active set optimization procedure***

## I. INTRODUCTION

A useful tool for anaerobic digestion (AD) process understanding and optimization is numerical simulation by using mechanistically inspired mathematical models. Till today, various mechanistically inspired AD models, ADM1 [1-6] and BioModel [7-13] based models, were developed containing various number of unknown or hardly determined AD model parameters, such are biochemical, kinetic, physicochemical, and stoichiometric model parameters. As the number of model parameters increases by expanding mathematical models, the efficiency and reliability of the calibration procedure typically decreases. Therefore, various procedures to reduce the number of the model parameters, which has to be calibrated, were proposed. In general, these procedures are based on adequate sensitivity analysis or similar approaches to calibrate various number of model parameters [13-21]. For example, Ahmed & Rodríguez [22] proposed the combined correlation-based parameter estimation with a sensitivity-based hierarchical and sequential single parameter optimization for sulfate reduction process by using the ADM1 model, while Kegl & Kovač Kralj [12] used an active set optimization (ASO) procedure combined with a gradient-based optimization algorithm in order to calibrate 113 model parameters of a BioModel.

In this paper attention is focused on the modeling of the AD process of a full-scale biogas plant by using a BioModel. More precisely, the focus is on the calibration of its 178 unknown design parameters by engaging the ASO procedure. A comparison of the daily dynamics of the predicted and measured AD performance as well as statistical indicators show that all 178 AD parameters (13 feedstock and 165 model parameters) can be successfully and efficiently calibrated by the engaged ASO procedure.

## II. BIOGAS PLANT EXPERIMENTAL DATA

The operation data used for AD simulation input and model calibration were obtained from a full-scale biogas plant Draženci (Slovenia). This plant consists of two equal mesophilic continuously mixed reactors (CSTRs). Both single-stage CSTRs have a hold up of 2500 $m^3$ with one common gas storage facility of 2500 $m^3$. The daily variation of total loading rate of the complex substrate (F-CS), temperature, and pH value in the CSTRs for a total period of two years are presented in Figure 1. The AD process with a retention time of approximately 33 days takes place at a constant pressure of 1.006 bar. The F-CS consists of poultry manure (PM), corn silage (CS), corn meal (CM), fat matter (FM), food waste (FW), and added water (W). The daily variations of fractions of CM, FM, FW, PM, CS, and W in the F-CS are shown for a total period of two years in Figure 2 and Figure 3. The composition of each substrate of F-CS containing TS-total solid, OM-organic matter, ch-carbohydrates, pr-proteins, li-lipids, $C_{io}$, $N_{io}$, $S_{io}$, $K_{io}$, and $P_{io}$ - inorganic carbon, nitrogen, sulfur, potassium, and phosphorus, and other elements and compounds, Table 1, was determined by the usage of methods prescribed in the corresponding standards.

*IEECP'22, July 21-22, 2022, Oxford, United Kingdom*

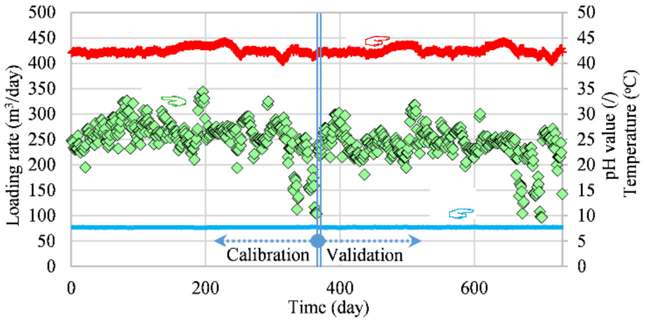


*Figure 1. Measured loading rate of F-CS and AD conditions.*

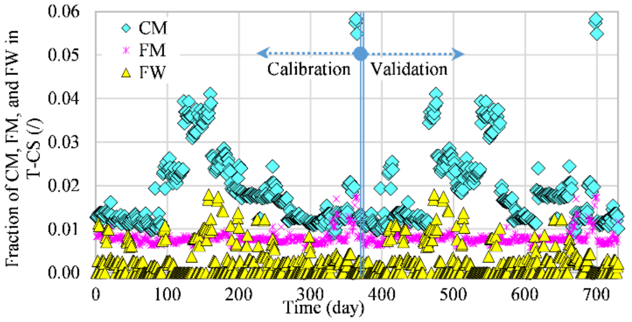


*Figure 2. Measured fractions of CM, FM, and FW in F-CS.*

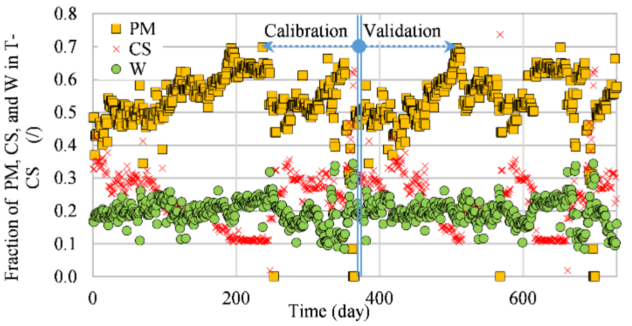


*Figure 3. Measured fractions of PM, CS, and W in F-CS.*

**Table 1. Composition of substrates in F-CS**

| F-CS | PM | CS | CM | FM | FW |
|---|---|---|---|---|---|
| TS (%) | 75.73 | 47.68 | 65.85 | 34.12 | 91.99 |
| OM (% TS) | 84.76 | 96.58 | 98.35 | 98.00 | 98.08 |
| ch ($gL^{-1}$) | 10.735 | 6.488 | 6.438 | 4.309 | 31.707 |
| pr ($gL^{-1}$) | 45.936 | 33.022 | 56.970 | 74.723 | 66.220 |
| li ($gL^{-1}$) | 3.555 | 3.226 | 19.750 | 236.312 | 26.970 |
| $C_{io}$ ($gL^{-1}$) | 3.57499 | 2.14185 | 0.71529 | 0.13711 | 42.80220 |
| $N_{io}$ ($gL^{-1}$) | 1.55322 | 0.62786 | 1.08176 | 1.30420 | 1.15234 |
| $S_{io}$ ($gL^{-1}$) | 3.57599 | 0.06147 | 0.37446 | 0.00100 | 0.98493 |
| $K_{io}$ ($gL^{-1}$) | 3.23805 | 1.10575 | 1.13509 | 0.04708 | 2.51013 |
| $P_{io}$ ($gL^{-1}$) | 2.61164 | 1.01155 | 3.54957 | 0.90058 | 6.63018 |
| Ca ($gL^{-1}$) | 3.61388 | 0.18493 | 0.02899 | 1.56674 | 18.09087 |
| Cr ($gL^{-1}$) | 0.00346 | 0.00026 | 0.00083 | 0.00250 | 0.00111 |
| Cu ($gL^{-1}$) | 0.00991 | 0.00035 | 0.00083 | 0.00238 | 0.01258 |
| Fe ($gL^{-1}$) | 0.11026 | 0.00542 | 0.01380 | 0.20543 | 0.27517 |
| Mg ($gL^{-1}$) | 0.81457 | 0.10843 | 0.30957 | 0.06587 | 0.88034 |
| Na ($gL^{-1}$) | 0.38816 | 0.00055 | 0.00746 | 0.06184 | 0.50550 |
| $NO_2$ ($gL^{-1}$) | 0.00871 | 0.00025 | 0.00175 | 0.00003 | 0.00048 |
| Ni ($gL^{-1}$) | 0.00052 | 0.00026 | 0.00083 | 0.00110 | 0.00111 |
| Pb ($gL^{-1}$) | 0.00028 | 0.00026 | 0.00083 | 0.00067 | 0.00111 |
| Zn ($gL^{-1}$) | 0.05228 | 0.00026 | 0.00535 | 0.02188 | 0.13295 |

To reduce the production of $H_2S$ during the AD process, the Kemira BDP-840 additive, containing the $FeCl_2$, in the amount of 100 L/day is added daily to the F-CS.

The total measured unrefined biogas volume is 4720983 $m^3$ in the first year, and 4364544 $m^3$ in the second year. This biogas contains approximately 54% $CH_4$, 45% $CO_2$, 60 ppm of $H_2$, 200 ppm of $H_2S$, and 800 ppm of $NH_3$. For the two years of observation, the measured daily produced biogas and $CH_4$ flow rates are presented in Figure 4, while $H_2$ and $H_2S$ flow rates are given in Figure 5.

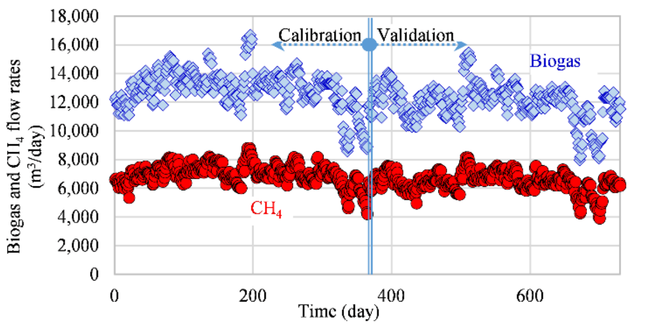


*Figure 4. Measured biogas and $CH_4$ flow rates in the biogas plant.*

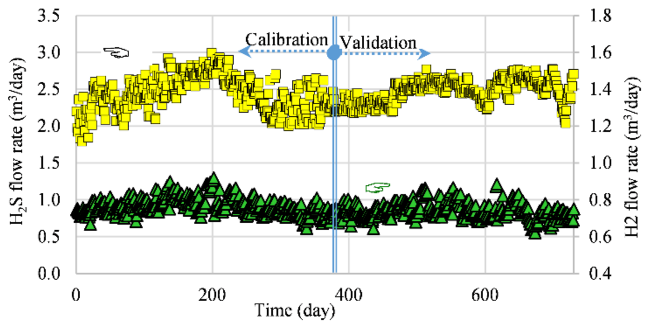


*Figure 5. Measured $H_2$ and $H_2S$ flow rates in the biogas plant.*

The daily variations of the shown data, measured at the plant during the first 365 days period, were used to calibrate the feedstock and model parameters of the proposed BioModel, while the measured data of the second year were used for BioModel validation.

## III. BIOMODEL PARAMETERS CALIBRATION

In order to calibrate a large number of design parameters (feedstock and model parameters) belonging to the BioModel, the ASO procedure is used in this work. In general, the employed ASO procedure involves the BioModel for numerical simulation of the AD process, a sensitivity analysis for determination of the active design variables from the set of all included design parameters, and an optimal design procedure.

### *A.* BioModel

The used mathematical model in this paper is of a BioModel-type [12], where biochemical and physicochemical processes during AD, considering the degradation of carbohydrates, proteins, and lipids into $CH_4$ and many other by-products, are described by the system of 75 ordinary differential equations (ODEs) and 53 algebraic equations (AEs). Physicochemical processes are related to (i) liquid-gas mass transfer for the set of biogas compounds $I_{gas} = \{CH_4, CO_2, H_2, H_2S, NH_3\}$ and to (ii) liquid-solid mass transfers for the set of precipitates $I_{prec} = \{CaCO_3, MgCO_3, FeCO_3, NiCO_3, CuCO_3, PbCO_3, ZnCO_3, FeS, CuS, NiS, PbS, ZnS, Ca_3(PO_4)_2, Fe_3(PO_4)_2, Ni_3(PO_4)_2, MgNH_4PO_4, KMgPO_4\}$. The BioModel includes a set of 178 design parameters as follows: (i) initial concentrations of 13 bacteria types from the set of $I_{\mathrm{bac}}$; acidogenic degraders of sugar, amino acids, glycerol, and oleic acid ($X_{\mathrm{Asu}}$, $X_{\mathrm{Aaa}}$, $X_{\mathrm{Agly}}$, and $X_{\mathrm{Aoa}}$), acetogenic degraders of propionic acid, butyric acid, and valeric acid ($X_{\mathrm{Apro}}$, $X_{\mathrm{Abu}}$, $X_{\mathrm{Ava}}$), methanogenic degraders of acetate and hydrogen ($X_{\mathrm{Mac}}$ and $X_{\mathrm{Mhyd}}$) sulfate reducing bacteria involving in reduction of sulfates ($X_{\mathrm{Ss}}$), and competing for propionate, acetate, and hydrogen ($X_{\mathrm{Spro}}$, ($X_{\mathrm{Sac}}$, and $X_{\mathrm{Shyd}}$; (ii) 3 hydrolysis rate constant: for carbohydrates, proteins, and lipids ($k_{\mathrm{hyd,ch}}$, $k_{\mathrm{hyd,pr}}$, $k_{\mathrm{hyd,li}}$); (iii) 26 inhibition constants; VFA inhibition of hydrolysis process ($K_{\mathrm{i,VFA}}$) and inhibitions of various compounds and metals ions on various bacteria growth ($K_{\mathrm{i,H_2,Agly}}$, $K_{\mathrm{i,H_2,Aoa}}$, $K_{\mathrm{i,H_2,Apro}}$, $K_{\mathrm{i,H_2S,Apro}}$, $K_{\mathrm{i,H_2,Abu}}$, $K_{\mathrm{i,H_2S,Abu}}$, $K_{\mathrm{i,H_2,Ava}}$, $K_{\mathrm{i,H_2S,Ava}}$, $K_{\mathrm{i,H_2S,Mac}}$, $K_{\mathrm{i,NH_3,Mac}}$, $K_{\mathrm{i,Cu^{2+},Abu}}$, $K_{\mathrm{i,Zn^{2+},Abu}}$, $K_{\mathrm{i,Cr^{2+},Abu}}$, $K_{\mathrm{i,Pb^{2+},Abu}}$, $K_{\mathrm{i,Ni^{2+},Abu}}$, $K_{\mathrm{i,Cu^{2+},Mac}}$, $K_{\mathrm{i,Zn^{2+},Mac}}$, $K_{\mathrm{i,Cr^{2+},Mac}}$, $K_{\mathrm{i,Pb^{2+},Mac}}$, $K_{\mathrm{i,Ni^{2+},Mac}}$, $K_{\mathrm{i,H_2S,Mhyd}}$, $K_{\mathrm{i,H_2S,Ss}}$, $K_{\mathrm{i,H_2S,Spro}}$, $K_{\mathrm{i,H_2S,Sac}}$, and $K_{\mathrm{i,H_2S,Shyd}}$); (iv) 2 limitation factors of inorganic nitrogen and inorganic phosphorus ($K_{\mathrm{M,N_{io}}}$ and $K_{\mathrm{M,P_{io}}}$) to all microbial growth rates and 16 Monod saturation constants including various substrates and bacteria ($k_{\mathrm{M,suAsu}}$, $k_{\mathrm{M,aaAaa}}$, $k_{\mathrm{M,glyAgly}}$, $k_{\mathrm{M,oaAoa}}$, $k_{\mathrm{M,proApro}}$, $k_{\mathrm{M,buAbu}}$, $k_{\mathrm{M,vaAva}}$, $k_{\mathrm{M,H_2Mhyd}}$, $k_{\mathrm{M,acMac}}$, $k_{\mathrm{M,Sio,atSs}}$, $k_{\mathrm{M,proSpro}}$, $k_{\mathrm{M,Sio,atSpro}}$, $k_{\mathrm{M,acSac}}$, $k_{\mathrm{M,Sio,atSac}}$, $\mathrm{k_{M,H_2Shyd}}$, $k_{\mathrm{M,Sio,atShyd}}$), (v) maximal microbial grow rates at optimal temperature for each of the 13 bacteria types $\mu_{i,\max,T_{\mathrm{opt}}}$, $i \in I_{\mathrm{bac}}$, microbial decays as a percentage of maximal microbial growth rates for each of 13 bacteria types $b_{i,\mathrm{dec}}$, $i \in I_{\mathrm{bac}}$, (vi) 10 parameters of mass transfer rates from liquid to gas phase, $(K_{\mathrm{L}}a)_{j,\mathrm{a}}$ and $(K_{\mathrm{L}}a)_{j,\mathrm{b}}$, $j \in I_{\mathrm{gas}}$; (vii) 17 precipitation rate constants $k_{\mathrm{cryst},k}$, $k \in I_{\mathrm{prec}}$; (viii) 65 parameters related to the determination of the bacteria growth rate of various microbial groups; $\mathrm{pK}_i^{\mathrm{lo}}$, $\mathrm{pK}_i^{\mathrm{up}}$, $\alpha_i$, $T_{i,\mathrm{opt}}$, and $T_{i,\max}$, $i \in I_{\mathrm{bac}}$. These parameters are treated as design parameters and are assembled into the vector $\mathbf{x}$.

## *B.* Sensitivity analysis

In the scope of the sensitivity analysis, a set $S_{\mathbf{x}}$ of random AD model designs $\mathbf{x}_j, j = 1, \dots N_S$ (each design $\mathbf{x}_j$ is a complete set of design parameters) is generated. Here, a set of $N_S = 5 \times 178 = 890$ random designs was used, since numerical experience has shown that such a sample was statistically representative enough. For each design $\mathbf{x}_j$ from the set $S_{\mathbf{x}}$ the derivatives $\frac{\partial g_0}{\partial x_i}$ of the objective function are computed. The objective function $g_0$, Eq. (1), was used for this purpose since it was defined as a high-quality measure of deviation between numerical simulation (NS) and actual measured biogas plant data.

$$g_0 = \psi_{0,1} \int_{t_{\mathrm{stab}}}^{t_{\mathrm{total}}} \left( \frac{Q_{\mathrm{biogas}}(t) - Q_{\mathrm{biogas,exp}}(t)}{\bar{Q}_{\mathrm{biogas,exp}}} \right)^2 dt + \psi_{0,2} \int_{t_{\mathrm{stab}}}^{t_{\mathrm{total}}} \left( \frac{Q_{\mathrm{g,CH_4}}(t) - Q_{\mathrm{g,CH_4,exp}}(t)}{\bar{Q}_{\mathrm{g,CH_4,exp}}} \right)^2 dt + \psi_{0,3} \int_{t_{\mathrm{stab}}}^{t_{\mathrm{total}}} \left( \frac{Q_{\mathrm{g,H_2}}(t) - Q_{\mathrm{g,H_2,exp}}(t)}{\bar{Q}_{\mathrm{g,H_2,exp}}} \right)^2 dt + \psi_{0,4} \int_{t_{\mathrm{stab}}}^{t_{\mathrm{total}}} \left( \frac{Q_{\mathrm{g,H_2S}}(t) - Q_{\mathrm{g,H_2S,exp}}(t)}{\bar{Q}_{\mathrm{g,H_2S,exp}}} \right)^2 dt + \psi_{0,5} \int_{t_{\mathrm{stab}}}^{t_{\mathrm{total}}} \left( \frac{\mathrm{pH}(t) - \mathrm{pH_{exp}}(t)}{\overline{\mathrm{pH}}_{\mathrm{exp}}} \right)^2 dt \quad (1)$$

where $\psi_{0,1}$, $\psi_{0,2}$, $\psi_{0,3}$, $\psi_{0,4}$, and $\psi_{0,5}$ are normalized weighting factors used to scale the relative importance of individual deviations, while $Q_{\mathrm{biogas}}(t)$, $Q_{\mathrm{g,CH_4}}(t)$, $Q_{\mathrm{g,H_2}}(t)$, $Q_{\mathrm{g,H_2S}}(t)$, $Q_{\mathrm{biogas,exp}}(t)$, $Q_{\mathrm{g,CH_4,exp}}(t)$, $Q_{\mathrm{g,H_2,exp}}(t)$, $Q_{\mathrm{g,H_2S,exp}}(t)$, $\bar{Q}_{\mathrm{biogas,exp}}$, $\bar{Q}_{\mathrm{g,CH_4,exp}}$, $\bar{Q}_{\mathrm{g,H_2,exp}}$, $\bar{Q}_{\mathrm{g,H_2S,exp}}$ are time dependent predicted, time dependent measured, and average values of the measured biogas, $CH_4$, $H_2$, and $H_2S$ flow rates, respectively. Meanwhile, $\mathrm{pH}(t)$, $\mathrm{pH_{exp}}(t)$, and $\overline{\mathrm{pH}}_{\mathrm{exp}}$ denote time dependent predicted, time dependent measured, and the average values of the measured pH value.

The obtained results of sensitivity analysis are normalized so that $\max_i \left( \left| \frac{\partial g_0}{\partial x_i} \right| \right) = 1$ for each $\mathbf{x}_j$. For each design parameter $x_i$ the average absolute value $f_{\mathrm{AA},i}$ and variance $f_{\mathrm{VA},i}$ of the normalized $\frac{\partial g_0}{\partial x_i}$ with respect to the whole set $S_{\mathbf{x}}$ are computed. The normalized values of $f_{\mathrm{AA},i}$ and $f_{\mathrm{VA},i}$ are used to define the importance factor $f_{\mathrm{IM},i} = \frac{1}{2} f_{\mathrm{VA},i} + \frac{1}{2} f_{\mathrm{AA},i}$ of the design parameter $x_i$.

## *C.* Optimal design procedure

The multi-objective optimization problem is reformulated into a single-objective function $g_0$ by summing all considered deviations, multiplied by adequate weighting factors, Eq. (1).

The optimal design problem can be defined by Eq. (2)-(4).

$$\max g_0(\mathbf{x}, \mathbf{q}) \quad (2)$$

subject to constraints

$$g_i(\mathbf{x}, \mathbf{q}) \le 0, \qquad i = 1, \dots, k^* \quad (3)$$

and the response equation

$$h(\mathbf{x}, \mathbf{q}, \dot{\mathbf{q}}, t) = 0 \quad (4)$$

where the vector $\mathbf{x} \in R^{n^*}$ of design variables represents the set of all AD parameters of the BioModel. The vector $\mathbf{q} \in R^{m^*}$ assembles the response variables describing the response of the AD system and $\dot{\mathbf{q}} \in R^{m^*}$ are their first time derivatives. The response equation, Eq. (4), establishes the dependency of $\mathbf{q}$ on $t$ and $\mathbf{x}$ and is given by the BioModel described in [12]. The scalar functions $g_0$ and $g_i$ are termed the objective and constraint functions, respectively. The objective function is related to the quality of AD performance, while the constraints reflect the imposed limitations. The constraint functions in the standard form, Eq. (3), are related to the maximal allowed initial concentration of all bacteria group and to the allowed range of the differences between measured and predicted values of the observed AD performance [12]. The symbol $n^*$ denotes the number of design variables, $k^*$ is the number of constraints and $m^*$ is the number of response variables.

## *D.* ASO procedure

The ASO procedure used to calibrate the values of a large number of design parameters is described in detail in [12]. In short, it consists of following two steps.

### *1) Identification and initialization of design variables*

In [12], the following 113 parameters are considered: the initial concentrations of the 13 types of bacteria in the F-CS, 3 hydrolysis rate constants, 26 inhibition constants, 2 limitation factors, 16 Monod saturation constants, maximal microbial grow rates at optimal temperature for each of the 13 bacteria types, microbial decays as a percentage of maximal microbial growth rates for each of 13 bacteria types, 10 parameters of mass transfer rates from liquid to gas phase, and 17 precipitation rate constants. In this paper, another 65 parameters, influencing the growth rate of 13 microbial groups $\mu_j$, $j \in I_{\mathrm{bac}}$ (parameters $\mathrm{pK}_i^{\mathrm{lo}}$, $\mathrm{pK}_i^{\mathrm{up}}$, $\alpha_i$, $T_{i,\mathrm{opt}}$, and $T_{i,\max}$, $i \in I_{\mathrm{bac}}$) are included. The normalized design variables are defined as: $x_i = \frac{(x_{\mathrm{P},i} - x_{\mathrm{P},i}^{\min})}{(x_{\mathrm{P},i}^{\max} - x_{\mathrm{P},i}^{\min})} \in [0,1]$, $i = 1 \dots n^*$, where $x_{\mathrm{P},i}$ is the $i^{\mathrm{th}}$ AD feedstock/model parameter, $x_{\mathrm{P},i}^{\min}$ and $x_{\mathrm{P},i}^{\max}$ are its lower an upper limits, and $n^* = 178$. The initial values of all design variables are set to the recommended values obtained from the literature.

### *2) Gradual optimization of design variables*

This step is performed in several cycles. Within each cycle, an adequate activation threshold value $f_T$ is chosen to select the active design variables $x_i^*$ for which it holds $f_{\mathrm{IM},i} \geq f_T$; all other design variables are designated as passive in the current cycle. After that, the optimal design problem, Eqs. (2)-(4), is solved in order to optimize the active design variables; for this purpose, a gradient-based algorithm with adaptive approximation scheme is engaged. This completes the current cycle. After that a new cycle with a lower activation threshold value is started. This procedure is continued until all design variables are active and optimized (calibrated).

# IV. RESULTS AND DISCUSSION

The proposed AD model and the whole optimization procedure were coded in-house in the C# language. The system of ODEs was solved by the Runge-Kutta method with an option to resort to the Euler method in case of (very rare) numerical instabilities. The engaged optimization algorithm is based on an approximation method [23-24] which sequentially generates approximate, strictly convex, and separable nonlinear programming problems and solves them to generate a sequence of converging approximate solutions. The algorithm uses the history of design derivatives of the objective and constraint functions to gradually improve the quality of the approximation. In this work numerical differentiation by using simple forward differences was used to get the needed design derivatives. Since there are 178 design variables, such derivatives computation is rather CPU intensive. To improve numerical performance, the computation of design derivatives was parallelized; this accelerated the computation by a factor practically equal to the number of CPU cores. In this scenario, one full optimization cycle (with all 178 design variables being active) took about 1 minute of CPU time on an 8-core i7 CPU desktop computer. The number of optimization cycles, needed to obtain optimum parameters, ranged usually up to 100.

In the following, the results of BioModel calibration are given as well as the results of the calibrated BioModel validation.

## *A.* BioModel calibration

During optimization the values of 178 design parameters (13 feedstock and 165 model parameters) were allowed to vary between lower and upper limits. Wherever possible, these limits were obtained by taking the smallest and largest values of those parameters as reported in the literature [3, 6, 12, 13, 15, 25-29]; the lower and upper limit values, $\mathrm{x}_{\mathrm{P},i}^{\min}$ and $\mathrm{x}_{\mathrm{P},i}^{\max}$, $i = 1 \dots n^*$, actually used in this work, are collected in Table 2.

In numerical simulation, the first 135 simulation days have been considered as a transient response or stabilization period, $t_{\mathrm{stab}}$, needed to reach steady state conditions for the input data corresponding to measured biogas plant data at day one. Therefore, in case of BioModel calibration, the comparison of the simulated and measured results was done only for the period of 365 days which follows the stabilization period of 135 days.

At the beginning, the value of 0.5 is used for the initial values of all normalized design variables $x_i$. During gradual optimization, the threshold values $f_T$ were sequentially chosen as 0.2 (Set1 1), 0.01 (Set 2), and 0.001 (Set 3). The corresponding number of active design variables $x_i^*$ increased from 7 (Set 1), through 24 (Set 2), up to 178 (Set 3). The optimized values of 7 active design variables, obtained in the optimization of Set 1, were kept as initial values of these variables for the optimization of the next set and so on. In Set 3 all design variables were included as the active design variables $x_i^*$ and the optimized values of all feedstock and model parameters are presented in Table 2.

The value of the objective function $g_0$ was gradually minimized from 9.685 (initial design) to 0.08575 (optimal design of Set 1 after 19 iterations), 0.0194 (optimal design of Set 2 after 31 iterations) to 0.0191 (optimal design of Set 3 after 60 iterations).

**Table 2. Feedstock and model parameters: lower, upper and optimized data.**

| $i$ | Parameter | $\mathrm{x}_{\mathrm{P},i}^{\min}$ | $\mathrm{x}_{\mathrm{P},i}^{\max}$ | Optimal value |
|---|---|---|---|---|
| 1 | $X_{\mathrm{Asu}}$ (gL$^{-1}$) | 0.1 | 0.5 | 0.29131 |
| 2 | $X_{\mathrm{Aaa}}$ (gL$^{-1}$) | 0.1 | 0.5 | 0.29092 |
| 3 | $X_{\mathrm{Agly}}$ (gL$^{-1}$) | 0.1 | 0.5 | 0.29108 |
| 4 | $X_{\mathrm{Aoa}}$ (gL$^{-1}$) | 0.1 | 0.5 | 0.29144 |
| 5 | $X_{\mathrm{Apro}}$ (gL$^{-1}$) | 0.1 | 0.5 | 0.30138 |
| 6 | $X_{\mathrm{Abu}}$ (gL$^{-1}$) | 0.1 | 0.5 | 0.30078 |
| 7 | $X_{\mathrm{Ava}}$ (gL$^{-1}$) | 0.1 | 0.5 | 0.29793 |
| 8 | $X_{\mathrm{Mac}}$ (gL$^{-1}$) | 0.1 | 0.5 | 0.30778 |
| 9 | $X_{\mathrm{Mhyd}}$ (gL$^{-1}$) | 0.1 | 0.5 | 0.10299 |
| 10 | $X_{\mathrm{Spro}}$ (gL$^{-1}$) | 0.1 | 0.5 | 0.28040 |
| 11 | $X_{\mathrm{Sac}}$ (gL$^{-1}$) | 0.1 | 0.5 | 0.29094 |
| 12 | $X_{\mathrm{Ss}}$ (gL$^{-1}$) | 0.1 | 0.5 | 0.29112 |
| 13 | $X_{\mathrm{Shyd}}$ (gL$^{-1}$) | 0.1 | 0.5 | 0.28475 |
| 14 | $k_{\mathrm{hyd,ch}}$ (day$^{-1}$) | 1.0 | 10.0 | 5.44266 |
| 15 | $k_{\mathrm{hyd,pr}}$ (day$^{-1}$) | 1.0 | 10.0 | 4.95942 |
| 16 | $k_{\mathrm{hyd,li}}$ (day$^{-1}$) | 1.0 | 10.0 | 5.01598 |
| 17 | $K_{\mathrm{i,VFA}}$ (gL$^{-1}$) | 0.1 | 0.6 | 0.22880 |
| 18 | $K_{\mathrm{i,H_2,Agly}}$ (gL$^{-1}$) | 0.01 | 0.1 | 0.05280 |
| 19 | $K_{\mathrm{i,H_2,Aoa}}$ (gL$^{-1}$) | 0.01 | 0.1 | 0.05280 |
| 20 | $K_{\mathrm{i,H_2,Apro}}$ (gL$^{-1}$) | 0.01 | 0.1 | 0.05284 |
| 21 | $K_{\mathrm{i,H_2,Abu}}$ (gL$^{-1}$) | 0.01 | 0.1 | 0.05280 |
| 22 | $K_{\mathrm{i,H_2,Ava}}$ (gL$^{-1}$) | 0.01 | 0.1 | 0.05279 |
| 23 | $K_{\mathrm{i,H_2S,Apro}}$ (gL$^{-1}$) | 0.1 | 0.9 | 0.48386 |
| 24 | $K_{\mathrm{i,H_2S,Abu}}$ (gL$^{-1}$) | 0.1 | 0.9 | 0.47729 |
| 25 | $K_{\mathrm{i,H_2S,Ava}}$ (gL$^{-1}$) | 0.1 | 0.9 | 0.47697 |
| 26 | $K_{\mathrm{i,H_2S,Mac}}$ (gL$^{-1}$) | 0.1 | 0.9 | 0.50035 |
| 27 | $K_{\mathrm{i,H_2S,Mhyd}}$ (gL$^{-1}$) | 0.1 | 0.9 | 0.46746 |
| 28 | $K_{\mathrm{i,H_2S,Ss}}$ (gL$^{-1}$) | 0.1 | 0.9 | 0.48012 |
| 29 | $K_{\mathrm{i,H_2S,Spro}}$ (gL$^{-1}$) | 0.1 | 0.9 | 0.48043 |
| 30 | $K_{\mathrm{i,H_2S,Sac}}$ (gL$^{-1}$) | 0.1 | 0.9 | 0.48051 |
| 31 | $K_{\mathrm{i,H_2S,Shyd}}$ (gL$^{-1}$) | 0.1 | 0.9 | 0.48081 |
| 32 | $K_{\mathrm{i,NH_3,Mac}}$ (gL$^{-1}$) | 0.1 | 0.3 | 0.22095 |
| 33 | $K_{\mathrm{i,Cu^{2+},Abu}}$ (gL$^{-1}$) | 0.1 | 0.9 | 0.48041 |
| 34 | $K_{\mathrm{i,Zn^{2+},Abu}}$ (gL$^{-1}$) | 0.1 | 0.9 | 0.48038 |
| 35 | $K_{\mathrm{i,Cr^{2+},Abu}}$ (gL$^{-1}$) | 0.1 | 0.9 | 0.48008 |
| 36 | $K_{\mathrm{i,Pb^{2+},Abu}}$ (gL$^{-1}$) | 0.1 | 0.9 | 0.48041 |
| 37 | $K_{\mathrm{i,Ni^{2+},Abu}}$ (gL$^{-1}$) | 0.1 | 0.9 | 0.48041 |
| 38 | $K_{\mathrm{i,Cu^{2+},Mac}}$ (gL$^{-1}$) | 0.1 | 0.9 | 0.48044 |
| 39 | $K_{\mathrm{i,Zn^{2+},Mac}}$ (gL$^{-1}$) | 0.1 | 0.9 | 0.48052 |
| 40 | $K_{\mathrm{i,Cr^{2+},Mac}}$ (gL$^{-1}$) | 0.1 | 0.9 | 0.47892 |
| 41 | $K_{\mathrm{i,Pb^{2+},Mac}}$ (gL$^{-1}$) | 0.1 | 0.9 | 0.48042 |
| 42 | $K_{\mathrm{i,Ni^{2+},Mac}}$ (gL$^{-1}$) | 0.1 | 0.9 | 0.48042 |
| 43 | $K_{\mathrm{M,N_{io}}}$ (gL$^{-1}$) | 0.001 | 0.01 | 0.00528 |
| 44 | $K_{\mathrm{M,P_{io}}}$ (gL$^{-1}$) | 0.001 | 0.01 | 0.00527 |
| 45 | $k_{\mathrm{M,suAsu}}$ (gL$^{-1}$) | 0.1 | 0.9 | 0.47809 |
| 46 | $k_{\mathrm{M,aaAaa}}$ (gL$^{-1}$) | 0.1 | 0.9 | 0.47919 |
| 47 | $k_{\mathrm{M,glyAgly}}$ (gL$^{-1}$) | 0.1 | 0.9 | 0.47978 |
| 48 | $k_{\mathrm{M,oaAoa}}$ (gL$^{-1}$) | 0.1 | 0.9 | 0.47888 |
| 49 | $k_{\mathrm{M,proApro}}$ (gL$^{-1}$) | 0.01 | 0.1 | 0.04837 |
| 50 | $k_{\mathrm{M,buAbu}}$ (gL$^{-1}$) | 0.01 | 0.1 | 0.05169 |
| 51 | $k_{\mathrm{M,vaAva}}$ (gL$^{-1}$) | 0.01 | 0.1 | 0.05266 |
| 52 | $k_{\mathrm{M,H_2Mhyd}}$ (gL$^{-1}$) | 0.01 | 0.1 | 0.03533 |
| 53 | $k_{\mathrm{M,acMac}}$ (gL$^{-1}$) | 0.1 | 0.5 | 0.10038 |
| 54 | $k_{\mathrm{M,Sio,atSs}}$ (gL$^{-1}$) | 0.1 | 0.5 | 0.28649 |

| | | | | |
|---|---|---|---|---|
| 55 | $k_{M,proSpro}$ (gL$^{-1}$) | 0.1 | 0.5 | 0.29016 |
| 56 | $k_{M,Sio,atSpro}$ (gL$^{-1}$) | 0.1 | 0.5 | 0.29016 |
| 57 | $k_{M,acSac}$ (gL$^{-1}$) | 0.1 | 0.5 | 0.28999 |
| 58 | $k_{M,Sio,atSac}$ (gL$^{-1}$) | 0.1 | 0.5 | 0.28999 |
| 59 | $\mathrm{k}_{M,H_2Shyd}$ (gL$^{-1}$) | 0.01 | 0.1 | 0.05147 |
| 60 | $k_{M,Sio,atShyd}$ (gL$^{-1}$) | 0.01 | 0.1 | 0.05041 |
| 61 | $\mu_{Asu,max,T_{opt}}$ (day$^{-1}$) | 1.0 | 10.0 | 5.29994 |
| 62 | $\mu_{Aaa,max,T_{opt}}$ (day$^{-1}$) | 1.0 | 10.0 | 5.30838 |
| 63 | $\mu_{Agly,max,T_{opt}}$ (day$^{-1}$) | 1.0 | 10.0 | 5.28801 |
| 64 | $\mu_{Aoa,max,T_{opt}}$ (day$^{-1}$) | 1.0 | 10.0 | 5.30106 |
| 65 | $\mu_{Apro,max,T_{opt}}$ (day$^{-1}$) | 1.0 | 12.0 | 6.49033 |
| 66 | $\mu_{Abu,max,T_{opt}}$ (day$^{-1}$) | 1.0 | 10.0 | 5.22845 |
| 67 | $\mu_{Ava,max,T_{opt}}$ (day$^{-1}$) | 1.0 | 10.0 | 5.24772 |
| 68 | $\mu_{Mac,max,T_{opt}}$ (day$^{-1}$) | 1.0 | 20.0 | 10.86708 |
| 69 | $\mu_{Mhyd,max,T_{opt}}$ (day$^{-1}$) | 1.0 | 10.0 | 5.40755 |
| 70 | $\mu_{Ss,max,T_{opt}}$ (day$^{-1}$) | 1.0 | 10.0 | 5.26495 |
| 71 | $\mu_{Spro,max,T_{opt}}$ (day$^{-1}$) | 1.0 | 10.0 | 5.28305 |
| 72 | $\mu_{Sac,max,T_{opt}}$ (day$^{-1}$) | 1.0 | 10.0 | 5.28666 |
| 73 | $\mu_{Shyd,max,T_{opt}}$ (day$^{-1}$) | 1.0 | 10.0 | 5.28801 |
| 74 | $b_{dec,Asu}$ (/) | 0.01 | 0.05 | 0.02899 |
| 75 | $b_{dec,Aaa}$ (/) | 0.01 | 0.05 | 0.02907 |
| 76 | $b_{dec,Agly}$ (/) | 0.01 | 0.05 | 0.02902 |
| 77 | $b_{dec,Aoa}$ (/) | 0.01 | 0.05 | 0.02903 |
| 78 | $b_{dec,Apro}$ (/) | 0.01 | 0.05 | 0.02783 |
| 79 | $b_{dec,Abu}$ (/) | 0.01 | 0.05 | 0.02827 |
| 80 | $b_{dec,Ava}$ (/) | 0.01 | 0.05 | 0.02880 |
| 81 | $b_{dec,Mac}$ (/) | 0.01 | 0.05 | 0.01001 |
| 82 | $b_{dec,Mhyd}$ (/) | 0.01 | 0.05 | 0.01253 |
| 83 | $b_{dec,Ss}$ (/) | 0.01 | 0.05 | 0.02914 |
| 84 | $b_{dec,Spro}$ (/) | 0.01 | 0.05 | 0.02903 |
| 85 | $b_{dec,Sac}$ (/) | 0.01 | 0.05 | 0.02902 |
| 86 | $b_{dec,Shyd}$ (/) | 0.01 | 0.05 | 0.02808 |
| 87 | $(K_La)_{CO_2,a}$ (°C$^{-1}$day$^{-1}$) | 1.0 | 5.0 | 2.89764 |
| 88 | $(K_La)_{CO_2,b}$ (day$^{-1}$) | 10.0 | 20.0 | 14.75347 |
| 89 | $(K_La)_{CH_4,a}$ (°C$^{-1}$day$^{-1}$) | 1.0 | 5.0 | 2.90732 |
| 90 | $(K_La)_{CH_4,b}$ (day$^{-1}$) | 10.0 | 20.0 | 14.75598 |
| 91 | $(K_La)_{H_2,a}$ (°C$^{-1}$day$^{-1}$) | 0.0001 | 0.001 | 0.00034 |
| 92 | $(K_La)_{H_2,b}$ (day$^{-1}$) | 0.001 | 0.01 | 0.00510 |
| 93 | $(K_La)_{H_2S,a}$ (°C$^{-1}$day$^{-1}$) | 0.0001 | 0.001 | 0.00010 |
| 94 | $(K_La)_{H_2S,b}$ (day$^{-1}$) | 0.001 | 0.01 | 0.00281 |
| 95 | $(K_La)_{NH_3,a}$ (°C$^{-1}$day$^{-1}$) | 0.0001 | 0.001 | 0.00053 |
| 96 | $(K_La)_{NH_3,b}$ (day$^{-1}$) | 0.001 | 0.01 | 0.00528 |
| 97 | $k_{cryst,CaCO_3}$ (day$^{-1}$) | 5.0 | 10.0 | 7.42617 |
| 98 | $k_{cryst,MgCO_3}$ (day$^{-1}$) | 5.0 | 10.0 | 7.37970 |
| 99 | $k_{cryst,FeCO_3}$ (day$^{-1}$) | 5.0 | 10.0 | 7.42335 |
| 100 | $k_{cryst,NiCO_3}$ (day$^{-1}$) | 5.0 | 10.0 | 7.37760 |
| 101 | $k_{cryst,CuCO_3}$ (day$^{-1}$) | 5.0 | 10.0 | 7.37770 |
| 102 | $k_{cryst,PbCO_3}$ (day$^{-1}$) | 5.0 | 10.0 | 7.37759 |
| 103 | $k_{cryst,ZnCO_3}$ (day$^{-1}$) | 5.0 | 10.0 | 7.37813 |
| 104 | $k_{cryst,FeS}$ (day$^{-1}$) | 50.0 | 100.0 | 73.74520 |
| 105 | $k_{cryst,NiS}$ (day$^{-1}$) | 50.0 | 100.0 | 73.77575 |
| 106 | $k_{cryst,CuS}$ (day$^{-1}$) | 50.0 | 100.0 | 73.77565 |
| 107 | $k_{cryst,PbS}$ (day$^{-1}$) | 50.0 | 100.0 | 73.77575 |
| 108 | $k_{cryst,ZnS}$ (day$^{-1}$) | 50.0 | 100.0 | 73.77525 |
| 109 | $k_{cryst,Ca_3(PO_4)_2}$ (day$^{-1}$) | 50.0 | 100.0 | 73.79385 |
| 110 | $k_{cryst,Fe_3(PO_4)_2}$ (day$^{-1}$) | 50.0 | 100.0 | 73.76085 |
| 111 | $k_{cryst,Ni_3(PO_4)_2}$ (day$^{-1}$) | 50.0 | 100.0 | 73.77580 |
| 112 | $k_{cryst,MgNH_4PO_4}$ (day$^{-1}$) | 100.0 | 200.0 | 147.87560 |
| 113 | $k_{cryst,K\,MgPO_4}$ (day$^{-1}$) | 50.0 | 100.0 | 73.84320 |
| 114 | $pK^{lo}_{Asu}$ (/) | 4.5 | 5.5 | 4.97564 |
| 115 | $pK^{up}_{Asu}$ (/) | 7.5 | 8.5 | 7.97649 |
| 116 | $pK^{lo}_{Aaa}$ (/) | 4.5 | 5.5 | 4.97558 |
| 117 | $pK^{up}_{Aaa}$ (/) | 7.5 | 8.5 | 7.97601 |
| 118 | $pK^{lo}_{Agly}$ (/) | 4.5 | 5.5 | 4.97555 |
| 119 | $pK^{up}_{Agly}$ (/) | 7.5 | 8.5 | 7.97580 |
| 120 | $pK^{lo}_{Aoa}$ (/) | 4.5 | 5.5 | 4.97560 |
| 121 | $pK^{up}_{Aoa}$ (/) | 7.5 | 8.5 | 7.97621 |
| 122 | $pK^{lo}_{Apro}$ (/) | 5.5 | 6.5 | 5.97771 |
| 123 | $pK^{up}_{Apro}$ (/) | 8.0 | 9.0 | 8.48162 |
| 124 | $pK^{lo}_{Abu}$ (/) | 5.5 | 6.5 | 5.97646 |
| 125 | $pK^{up}_{Abu}$ (/) | 8.0 | 9.0 | 8.48030 |
| 126 | $pK^{lo}_{Ava}$ (/) | 5.5 | 6.5 | 5.97590 |
| 127 | $pK^{up}_{Ava}$ (/) | 8.0 | 9.0 | 8.47841 |
| 128 | $pK^{lo}_{Mac}$ (/) | 5.5 | 6.5 | 5.97397 |
| 129 | $pK^{up}_{Mac}$ (/) | 8.0 | 9.0 | 8.49239 |
| 130 | $pK^{lo}_{Mhyd}$ (/) | 5.5 | 6.5 | 5.97724 |
| 131 | $pK^{up}_{Mhyd}$ (/) | 8.0 | 9.0 | 8.47170 |
| 132 | $pK^{lo}_{Ss}$ (/) | 5.5 | 6.5 | 5.97527 |
| 133 | $pK^{up}_{Ss}$ (/) | 7.5 | 8.5 | 7.97432 |
| 134 | $pK^{lo}_{Spro}$ (/) | 5.5 | 6.5 | 5.97553 |
| 135 | $pK^{up}_{Spro}$ (/) | 7.5 | 8.5 | 7.97556 |
| 136 | $pK^{lo}_{Sac}$ (/) | 5.5 | 6.5 | 5.97558 |
| 137 | $pK^{up}_{Sac}$ (/) | 7.5 | 8.5 | 7.97567 |
| 138 | $pK^{lo}_{Shyd}$ (/) | 5.5 | 6.5 | 5.97586 |
| 139 | $pK^{up}_{Shyd}$ (/) | 7.5 | 8.5 | 7.97696 |
| 140 | $\alpha_{Asu}$ (K$^{-1}$day$^{-1}$) | 0.00015 | 0.00019 | 0.00017 |
| 141 | $\alpha_{Aaa}$ (K$^{-1}$day$^{-1}$) | 0.00015 | 0.00019 | 0.00017 |
| 142 | $\alpha_{Agly}$ (K$^{-1}$day$^{-1}$) | 0.00015 | 0.00019 | 0.00017 |
| 143 | $\alpha_{Aoa}$ (K$^{-1}$day$^{-1}$) | 0.00015 | 0.00019 | 0.00017 |
| 144 | $\alpha_{Apro}$ (K$^{-1}$day$^{-1}$) | 0.00015 | 0.00019 | 0.00017 |
| 145 | $\alpha_{Abu}$ (K$^{-1}$day$^{-1}$) | 0.00016 | 0.00020 | 0.00018 |
| 146 | $\alpha_{Ava}$ (K$^{-1}$day$^{-1}$) | 0.00016 | 0.00020 | 0.00018 |
| 147 | $\alpha_{Mac}$ (K$^{-1}$day$^{-1}$) | 0.00015 | 0.00019 | 0.00017 |
| 148 | $\alpha_{Mhyd}$ (K$^{-1}$day$^{-1}$) | 0.00015 | 0.00019 | 0.00017 |
| 149 | $\alpha_{Ss}$ (K$^{-1}$day$^{-1}$) | 0.00016 | 0.00020 | 0.00018 |
| 150 | $\alpha_{Spro}$ (K$^{-1}$day$^{-1}$) | 0.00016 | 0.00020 | 0.00018 |
| 151 | $\alpha_{Sac}$ (K$^{-1}$day$^{-1}$) | 0.00016 | 0.00020 | 0.00018 |
| 152 | $\alpha_{Shyd}$ (K$^{-1}$day$^{-1}$) | 0.00016 | 0.00020 | 0.00018 |
| 153 | $T_{Asu,opt}$ (°C) | 50 | 60 | 54.75515 |
| 154 | $T_{Asu,max}$ (°C) | 60 | 70 | 64.75515 |
| 155 | $T_{Asa,opt}$ (°C) | 50 | 60 | 54.75515 |
| 156 | $T_{Aaa,max}$ (°C) | 60 | 70 | 64.75515 |
| 157 | $T_{Agly,opt}$ (°C) | 50 | 60 | 54.75515 |
| 158 | $T_{Agly,max}$ (°C) | 60 | 70 | 64.75515 |
| 159 | $T_{Aoa,opt}$ (°C) | 50 | 60 | 54.75515 |
| 160 | $T_{Aoa,max}$ (°C) | 60 | 70 | 64.75515 |
| 161 | $T_{Apro,opt}$ (°C) | 50 | 60 | 54.75513 |
| 162 | $T_{Apro,max}$ (°C) | 60 | 70 | 64.75515 |
| 163 | $T_{Abu,opt}$ (°C) | 55 | 65 | 59.75517 |
| 164 | $T_{Abu,max}$ (°C) | 65 | 75 | 69.75515 |
| 165 | $T_{Ava,opt}$ (°C) | 55 | 65 | 59.75516 |
| 166 | $T_{Ava,max}$ (°C) | 65 | 75 | 69.75515 |

| | | | | |
|---|---|---|---|---|
| 167 | $T_{Mac,opt}$ (°C) | 50 | 60 | 54.75522 |
| 168 | $T_{Mac,max}$ (°C) | 60 | 70 | 64.75515 |
| 169 | $T_{Mhyd,opt}$ (°C) | 50 | 60 | 54.75515 |
| 170 | $T_{Mhyd,max}$ (°C) | 60 | 70 | 64.75515 |
| 171 | $T_{Ss,opt}$ (°C) | 30 | 40 | 34.75274 |
| 172 | $T_{Ss,max}$ (°C) | 60 | 70 | 64.75389 |
| 173 | $T_{Spro,opt}$ (°C) | 30 | 40 | 34.75592 |
| 174 | $T_{Spro,max}$ (°C) | 60 | 70 | 64.75487 |
| 175 | $T_{Sac,opt}$ (°C) | 30 | 40 | 34.75672 |
| 176 | $T_{Sac,max}$ (°C) | 60 | 70 | 64.75518 |
| 177 | $T_{Shyd,opt}$ (°C) | 30 | 40 | 34.75631 |
| 178 | $T_{Shyd,max}$ (°C) | 60 | 70 | 64.75447 |

The biogas flow rates, obtained by simulation with the initial and various optimal values of design parameters (computed with active design variables from Sets 1 to Set 3 – optimal design), are compared to the measured data in Figure 6. The mean biogas flow rate, obtained with initial values of design parameters, differs on average from the measured values by around 6.5 % (average absolute daily difference divided by average daily measurement). By far the largest improvement of these results is reached by optimizing the active design variables of Set 1. Further optimization of the Set 2 and Set 3 gradually also improves the result but the improvements are becoming progressively small. It is clearly evident that the biogas flow rate obtained with the optimal (calibrated) values of all 178 design parameters, presented in Table 2, are the closest to the measured biogas rates. The simulated data of biogas flow rate agree very well with the measured values; the average difference is less than 0.1%. The total biogas volume, delivered by the biogas plant within 365 days, is by about 7% higher than the one computed with the initial values of design parameters. After optimization, this difference becomes practically negligible (less than 0.5%).

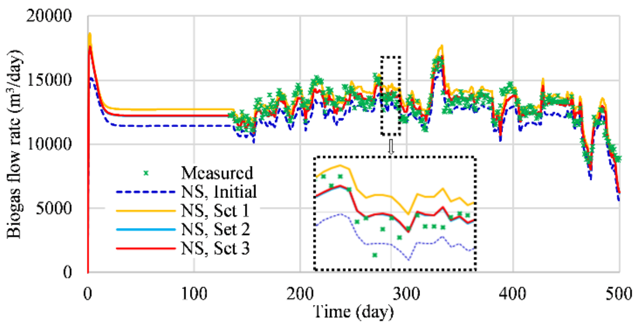


*Figure 6. Dynamics of biogas flow rate, BioModel calibration.*

The $CH_4$ flow rates, obtained numerically with the initial and the optimal values of design parameters from various sets, are compared to the measured data in Figure 7. Initially, the simulated $CH_4$ flow rate differs from the measured one by 9.4% on average. By optimizing the active design variables of Set 1, this difference is decreased substantially, while further improvements obtained by optimizing the design parameters from Set 2 and Set 3 are rather small, resulting in the final difference of approximately 1.2%. The total produced $CH_4$ volume, delivered by the plant within 365 days, is around 10% higher than the one computed with the initial values of design parameters. After the optimization, this difference is below 0.3%.

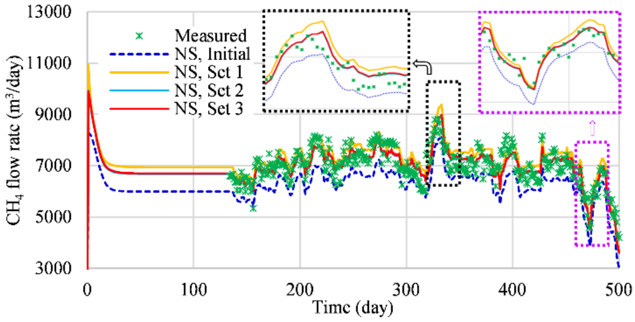


*Figure 7. Dynamics of $CH_4$ flow rate, BioModel calibration.*

The numerically obtained $H_2$ flow rate history is compared to measured data in Figure 8. It can be observed that the substantial difference between measured and simulation (initial design) decreased drastically after optimizing Set 1. Further optimization including more design parameters improves gradually the result. The average difference, which was initially approximately 138%, fell after optimizing Set 1 to about 8.6% and after optimizing Set 3 to 1%. With fully optimized design parameters, the computed total $H_2$ volume differs by around 0.1% from the measured data; initially this difference was around 138%.

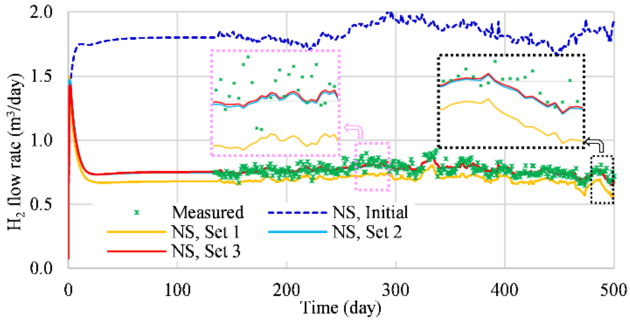


*Figure 8. Dynamics of $H_2$ flow rate, BioModel calibration.*

Figure 9 shows the comparison of dynamics of $H_2S$ flow rate, obtained by simulation and experiment. Similar to $H_2$ flow rate, it can be observed that the difference between measured and initial design is substantially. These differences are reduced significantly after optimizing the Set 1; however, little further progress can be observed after optimizing Set 2 and Set 3. Low values of $H_2S$ flow rate can be obtained by considering the Kemira BDP-840 additive, which contains $FeCl_2$ to reduce $H_2S$ content in the produced biogas. The average difference, which was initially approximately 535%, fell after optimizing the design variables of Set 3 to a negligible value. With fully optimized design parameters (Set 3), the computed total $H_2S$ volume differs by less than 0.1% from the measured data; initially this difference was over 539%.

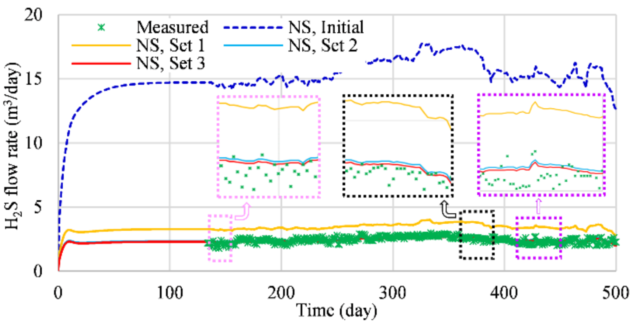


*Figure 9. Dynamics of $H_2S$ flow rate, BioModel calibration.*

The numerically obtained dynamics of pH values are compared to experimental data in Figure 10. It can be seen that after the stabilization period of 135 days, the optimal values of design parameters deliver a rather constant pH value very close to pH 7.7, which is the mean measured value. The average difference, which was initially approximately 4.5%, fell after optimizing the design variables of Set 3 to less than 0.3%.

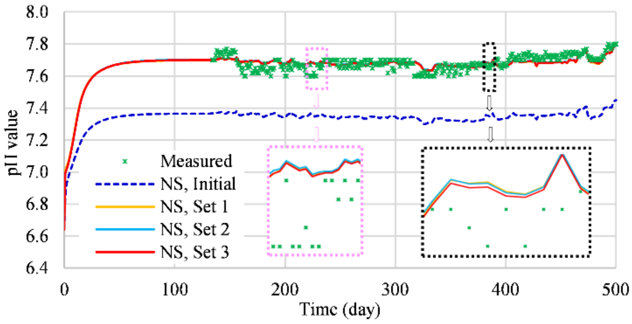


*Figure 10. Dynamics of* pH *value, BioModel calibration.*

According to the presented results, one can say that the optimization of the most important parameters (Set 2) yields relatively good results. For the fine tuning, however, the activation of all design parameters (Set 3, Optimal) may be worth a consideration.

## *B.* BioModel validation

The calibrated values of all 178 design parameters were validated by using another set of measured data from the same biogas plant. The comparison between measured and predicted values of pH value, biogas and $CH_4$ flow rates are given in Figure 11.

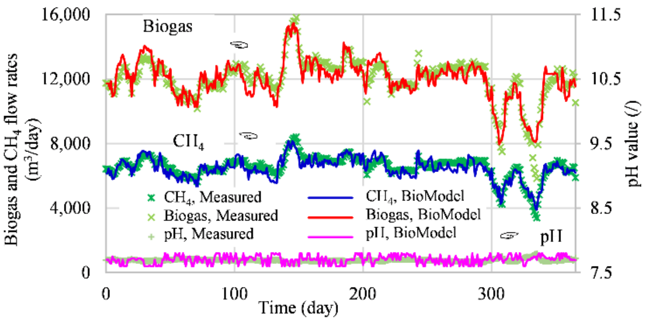


*Figure 11. Dynamics of biogas and* $CH_4$ *flow rates and* pH *value, BioModel validation.*

Figure 12 shows the dynamics of $H_2$ and $H_2S$ flow rates, obtained by measurements and simulation.

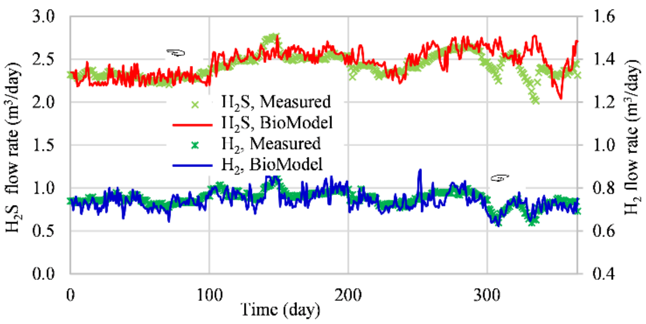


*Figure 12. Dynamics of* $H_2$ *and* $H_2S$ *flow rates, BioModel validation.*

From Figure 11 and Figure 12 it can be seen, that the dynamics of the predicted AD performances follow very well the dynamics of the measured AD performance through the 365 days. The agreement between all measured and predicted AD performances is quite good; therefore, it can be concluded that the calibrated values of all 178 design parameters by using the proposed ASO procedure enable satisfactory prediction of the AD process.

## *C.* Evaluation of the ASO procedure

For the evaluation of the proposed ASO procedure, the measured and predicted AD performances are estimated by two statistical indicators (SI): coefficient of determination ($R^2$), Eq. (5), and the relative index of agreement $I_{\mathrm{A,rel}}$, Eq. (6) [12, 30].

$$R^2 = \left( \frac{\sum_{i=1}^{n} |y_{\mathrm{exp},i} - \bar{y}_{\mathrm{exp}}| \, |y_{\mathrm{NS},i} - \bar{y}_{\mathrm{NS}}|}{\sqrt{\sum_{i=1}^{n} (y_{\mathrm{exp},i} - \bar{y}_{\mathrm{exp}})^2} \sqrt{\sum_{i=1}^{n} (y_{\mathrm{NS},i} - \bar{y}_{\mathrm{NS}})^2}} \right)^2 \tag{5}$$

$$I_{\mathrm{A,rel}} = 1 - \frac{\sum_{i=1}^{n} \left( \frac{y_{\mathrm{exp},i} - y_{\mathrm{NS},i}}{\bar{y}_{\mathrm{exp}}} \right)^2}{\sum_{i=1}^{n} \left( \frac{|y_{\mathrm{NS},i} - \bar{y}_{\mathrm{exp}}| + |y_{\mathrm{exp},i} - \bar{y}_{\mathrm{exp}}|}{\bar{y}_{\mathrm{exp}}} \right)^2} \tag{6}$$

where $n$ is the number of comparison points, $y_{\mathrm{exp},i}$ and $y_{\mathrm{NS},i}$ relate to the measured and predicted values of AD performance at $i^{\mathrm{th}}$ day of the AD process, respectively, while $\bar{y}_{\mathrm{exp}}$ and $\bar{y}_{\mathrm{NS}}$ are average values of the measured and predicted AD performance of the complete AD process, respectively.

The coefficient of determination $R^2$ and relative index of agreement $I_{\mathrm{A,rel}}$ in case of BioModel calibration and BioModel validation are given in Table 3.

**Table 3. Statistical indicators for ASO procedure**

| SI | Mode | Design | $Q_{CH_4}$ | $Q_{H_2}$ | $Q_{H_2S}$ | $Q_{\mathrm{biogas}}$ |
|---|---|---|---|---|---|---|
| $R^2$ | Calibration | Initial | 0.8215 | 0.4389 | 0.6073 | 0.8314 |
| | | Optimal | 0.8310 | 0.6459 | 0.5985 | 0.8324 |
| | Validation | | 0.8299 | 0.6130 | 0.6226 | 0.8616 |
| $I_{\mathrm{A,rel}}$ | Calibration | Initial | 0.7569 | 0.0663 | 0.0317 | 0.8514 |
| | | Optimal | 0.9350 | 0.8048 | 0.7582 | 0.9406 |
| | Validation | | 0.9352 | 0.7823 | 0.7455 | 0.9535 |

The obtained values of the statistical indicators confirm that the presented ASO procedure based on the included BioModel are reliable and efficient. It is clearly evident, that the optimization of all 178 parameters results in the improvement of the accuracy of simulation when compared with the BioModel containing only 113 design parameters [12].

# V. CONCLUSIONS

The agreement of the obtained results by numerical simulation of the AD process in a single CSTR of a full-scale biogas plant and the measured AD performance through the observed two years, confirms the efficiency of the used AD BioModel which takes into account the Kemira BDP-840 additive to reduce $H_2S$ content in the produced biogas. Furthermore, it is evident that the active set optimization procedure and the engaged gradient-based optimizer to calibrate all 178 feedstock and model parameters is reliable and efficient, especially, if the computation of design derivatives is parallelized.

# VI. ACKNOWLEDGMENTS

The author is grateful for the financial support of the Slovenian Research Agency (PhD research fellowship contract No. 1000-18-0552 and core research funding No. P2-0032). The author highly appreciates the collaboration with Biogas Plant Draženci for providing the necessary experimental data.

## VII. REFERENCES


[1] D. J. Batstone, J. Keller, I. Angelidaki, S. V. Kalyuzhnyi, S. G. Pavlostathis, A.Rozzi, W. T. M. Sanders, H. Siegrist, V. A. Vavilin, Anaerobic Digestion Model No. 1 (ADM1). London: IWA Publishing, 2002.

[2] A. Donoso-Bravo, D. Olivares, Y. Lesty, H. V. Bossche, "Explotation of the ADM1 in a XXI century wastewater resource recovery facility (WRRF): The case of codigestion and thermal hydrolysis." Water Research vol. 175, no. 115654, 2020.

[3] X. Flores-Alsina, K. Solon, C. K. Mbamba, S. Tait, K. V. Gernaey, U. Jeppsson, D. J. Batstone, "Modelling phosphorus (P), sulfur (S) and iron (Fe) interactions for dynamic simulations of anaerobic digestion processes," Water Research, vol. 95, pp. 370-382., 2016.

[4] L. Frunzo, F. G. Fermoso, V. Luongo, M. R. Mattei, G. Esposito, "ADM1-based mechanistic model for the role of trace elements in anaerobic digestion processes," Journal of Environmental Management, vol. 241, pp. 587-602, 2019.

[5] B. C. Maharaj, M. R. Mattei, L. Frunzo, E.D. van Hullebusch, G. Esposito, "ADM1 based mathematical model of trace element precipitation/dissolution in anaerobic digestion processes," Bioresource Technology, vol. 267, pp. 666-676, 2018.

[6] H. Sun, Z. Yang, Q. Zhao, M. Kurbonova, R. Zhang, G. Liu, W. Wang,, "Modification and extension of anaerobic digestion model No.1 (ADM1) for syngas biomethanation simulation: From lab-scale to pilot-scale," Chemical Engineering Journal, vol. 403, no. 126177, 2021.

[7] I. Angelidaki, L. Ellegaard, B. K. Ahring, "A mathematical model for dynamic simulation of anaerobic digestion of complex substrates: Focusing on ammonia inhibition," Biotechnology and Bioengineering vol. 42, pp. 159-166, 1993.

[8] I. Angelidaki, L. Ellegaard, B. K. Ahring, "A comprehensive model of anaerobic bioconversion of complex substrates to biogas," Biotechnology and Bioengineering , vol. 63(3), pp. 363-372, 1999.

[9] T. Fitamo, A. Boldrin, G. Dorini, K. Boe, I. Angelidaki, C. Scheutz, "Optimising the anaerobic co-digestion of urban organic waste using dynamic bioconversion mathematical modelling, " Water Research, vol. 106, pp. 283-294, 2016.

[10] T. Kegl, A. Kovač Kralj, "Multi-objective optimization of anaerobic digestion process using a gradient-based algorithm," Energy Conversion and Management, vol. 226, no. 113560, 2020.

[11] T. Kegl, T., A. Kovač Kralj, "Optimization of biogas production from cattle manure by anaerobic digestion using a gradient-based algorithm," Computer Aided Chemical Engineering, vol. 50, pp. 1909-1915, 2021.

[12] T. Kegl, A. Kovač Kralj, "An enhanced anaerobic digestion BioModel calibrated by parameters optimization based on measured biogas plant data," Fuel, vol. 322, no. 122984, 2022.

[13] A. Kovalovszki, M. Alvarado-Morales, I. A. Fotidis, I. Angelidaki, "A systematic methodology to extend the applicability of a bioconversion model for the simulation of various co-digestion scenarios," Bioresource Technology, vol. 235, pp. 157-166, 2017.

[14] K. Bułkowska, I. Białobrzewski, Z. Mariusz Gusiatin, E. Klimiuk, T. Pokoj, "ADM1-based modeling of anaerobic codigestion of maize silage and cattle manure – calibration of parameters and model verification (part II)," Archives of Environmental Protection, vol. 41, pp. 20-27, 2015.

[15] Z. Fatolahi, G. Arab, V. Razaviarani, "Calibration of the Anaerobic Digestion Model No. 1 for anaerobic digestion of organic fraction of municipal solid waste under mesophilic condition," Biomass and Bioenergy, vol. 139, no. 105661, 2020.

[16] A. Kovalovszki, L. Treu, L. Ellegaard, G. Luo, I. Angelidaki, "Modeling temperature response in bioenergy production: Novel solution to a common challenge of anaerobic digestion," Applied Energy, vol. 263, no. 114646, 2020.

[17] F. A. Neba, H. M. Tornyeviadzi, S. W. Østerhus, R. Seidu, "Self-optimizing attainable regions of the anaerobic treatment process: Modeling performance targets under kinetic uncertainty," Water Research, vol. 171, no. 115377, 2020.

[18] H. Ozgun, "Anaerobic Digestion Model No. 1 (ADM1) for mathematical modeling of full-scale sludge digester performance in a municipal wastewater treatment plant," Biodegradation, vol. 30, pp. 27-36, 2019.

[19] D. Poggio, M. Walker, W. Nimmo, L. Ma, M. Pourkashanian, "Modelling the anaerobic digestion of solid organic waste – Substrate characterisation method for ADM1 using a combined biochemical and kinetic parameter estimation approach," Waste Management, vol. 53, pp. 40-54, 2016.

[20] K. Postawa, J. Szczygiel, M. Kułażyński, "Heuristic methods in optimization of selected parameters of Two-Phase Anaerobic Digestion (TPAD) model," Fuel, vol. 281, no. 118257, 2020.

[21] D. P. Van, T. Fujiwara, B. L. Tho, P. P. S. Toan, G. H. Minh, "A review of anaerobic digestion systems for biodegradable waste: Configurations, operating parameters, and current trends," Environmental Engineering Research, vol. 25(1), pp. 1-17, 2020.

[22] W. Ahmed, J. Rodríguez, "Generalized parameter estimation and calibration for biokinetic models using correlation and single variable optimisations: Application to sulfate reduction modelling in anaerobic digestion," Water Research, vol. 122, pp. 407-418, 2017.

[23] M. Kegl, B. J. Butinar, B. Kegl, "An efficient gradient-based optimization algorithm for mechanical systems," Communications in Numerical Methods in Engineering, vol. 18, pp. 363-371, 2002.

[24] M. Kegl, M. M. Oblak, "Optimization of mechanical systems: on non-linear first-order approximation with an additive convex term," Communications in Numerical Methods in Engineering, vol. 13, pp. 13-20, 1997.

[25] D. J. Batstone, Y. Amerlinck, G. Ekam, R. Goel, P. Grau, B. Johnson, I. Kaya, J. P. Steyer, S. Tait, I. Takács, A. Vanrolleghem, C. J. Brouckaert, E. Volcke, "Towards a generalized physicochemical framework," Water Science & Technology , vol. 66(6), pp. 1147-1161, 2012.

[26] S. Jabłoński, M. Łukaszewicz, "Mathematical modelling of methanogenic reactor start-up: Importance of volatile fatty acids degrading population," Bioresource Technology, vol. 174, pp. 74-80, 2014.

[27] C. Kazadi Mbamba, D. J. Batstone, X. Flores-Alsina, "A generalised chemical precipitation modelling approach in wastewater treatment applied to calcite," Water Research, vol. 68, pp. 342-353, 2015.

[28] C. Kazadi Mbamba, S. Tait, X. Flores-Alsina, D. J. Batstone, "A systematic study of multiple minerals precipitation modelling in wastewater treatment," Water Research, vol. 85, pp. 359-370, 2015.

[29] A. Keshtkar, H. Ghaforian, G. Abolhamd, B. Meyssami, "Dynamic simulation of cyclic batch anaerobic digestion of cattle manure," Bioresource Technology, vol. 80, pp. 9-17., 2001.https://doi.org/10.1016/S0960-8524(01)00071-2

[30] V. Phogat, M. A. Skewes, J. Simunek, "Statistical assessment of a numerical model simulating agro hydrochemical processes in soil under drip fertigated mandarin tree," Irrigation & Drainage Systems Engineering, vol. 5, no.155, 2016.